Improved Spatially-Coupled Multiuser Transmission via Constellation Rotation

Min Jiang and Zhongwei Si
Key Laboratory of Universal Wireless Communications, Ministry of Education
Beijing University of Posts and Telecommunications, Beijing, China 100876
Email: {jmin, sizhongwei}@bupt.edu.cn

Abstract—**Spatial coupling has been applied in multiple access system in order to obtain higher spectral efficiency, where different users share the same resource blocks by superimposing data streams with different time offsets. In this paper, we introduce constellation rotation into the spatially-coupled multiuser system to further distinguish users and mitigate the interferences. The optimization of the rotation angles is carried out by maximizing the average mutual information between the transmitted symbols and the received signal. Simulation results show that the constellation rotation generally contributes to the performance improvement of the system and reduces the decoding latency. Benefiting from the optimization, the system with the optimal rotation angle set clearly outperforms the others.**

I. Introduction

With the growing demand, the fifth generation (5G) wireless communication faces many challenges including high spectral efficiency and massive connection. Conventional orthogonal multiple access (OMA) is difficult to meet the demand, whereas non-orthogonal multiple access (NOMA) [1] catches numerous attractions for its advantages in the resource allocation. In NOMA, data streams from different users are allowed to be superimposed, which makes the system achieve higher spectral efficiency. NOMA modulation [2], power allocation and user scheduling [3] are potential research directions to improve the system performance.

Spatial graph coupling is a method where a new graph is produced by randomly connecting the copies of a protograph. The technique was first applied to construct spatially-coupled low-density parity-check (LDPC) codes [4] which had been proven to reach the same threshold as the maximum *a posteriori* probability (MAP) decoding of the corresponding LDPC block codes [5]. Recently, applications of the method have been found in multiple access, where different users share the same resource blocks by superimposing different data streams with different time offsets. In [6], it has been proved that the spatial coupling theoretically achieves the capacity of the multiple access channel. Spatial coupling was used practically in the code-division multiple-access (CDMA) in [7] with iterative multiuser detection. A multiple access demodulation with lower complexity was proposed in [8] which obtains the same performance as its counterpart.

Spatially-coupled multiuser transmission achieves a good performance in theory, but in practice the interferences between different data streams of all users are difficult to distinguish only with the help of channel coding. The constellation rotation introduced in [9] provides a possibility for solving this problem. The constellation rotation contributes to increase the modulation diversity and is widely used to make a further distinction among the superimposed symbols. As an example, the multi-dimensional sparse code multiple access (SCMA) codebook design with constellation rotation proposed in [10] achieves a better performance.

In this paper, we introduce constellation rotation into the spatially-coupled multiuser transmission. Each data stream is channel-encoded and modulated before transmitting via additive white Gaussian noise (AWGN) channels. During the modulation, different data streams of the same user or all data streams of all users are modulated with different constellation rotations. In comparison to the existing methods, we increase the constellation diversity of the superimposed data and make a further distinction between different data streams. This is beneficial for the multiuser detection at the receiver. Furthermore, we search for the optimal rotation angle set by maximizing the average mutual information (AMI). The spatial coupling is carried out by superimposing the data streams with different time offsets. At the receiver, we employ iterative detection and decoding to recover the data. Based on the simulation results, we draw the conclusion that the constellation rotation contributes to the performance improvement of the system in terms of extrinsic information transfer (EXIT) charts and bit error rate (BER) curves.

The rest of the paper is organized as follows. In Section II, the system model of the spatially-coupled multiuser transmission is introduced. We make elaborated description on spatial coupling with constellation rotation, rotation angle optimization and the iterative detection and decoding algorithm in Section III. The simulation results and discussions are represented in Section IV with the help of EXIT charts and BER curves. Finally, Section V summarizes the paper.

II. System Model

The system model of the spatially-coupled multiuser transmission in this paper is shown in Fig. 1. We make assumptions that all users have the same numbers of data streams and packages, and each data stream is equal-power and independent. To simplify the description, we take $\mathbf{b}_{l,s}$ as an example, which represents the s-th data stream of user l,

978-1-5386-3531-5/17/$31.00 © 2017 IEEE

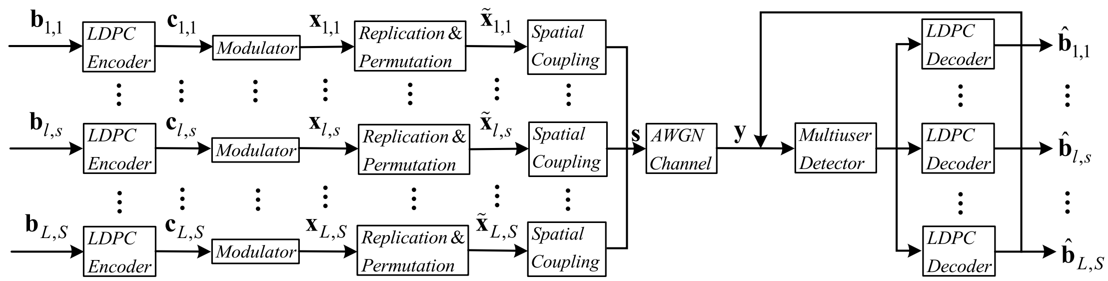

Fig. 1. The system model of spatially-coupled multiuser superposition transmission with L users and S data streams per user.

$l \in \{1, \cdots, L\}$, $s \in \{1, \cdots, S\}$, and L and S denote the number of user and the number of data streams per user, respectively. At the transmitter, binary information sequence $\mathbf{b}_{l,s} = \left[\mathbf{b}^T{}_{l,s,1}, \mathbf{b}^T{}_{l,s,2}, \cdots, \mathbf{b}^T{}_{l,s,P}\right]^T$ in P packages is encoded by LDPC encoders with code rate $R = K/N$, where sequence $\mathbf{b}_{l,s,p} = \left[b_{l,s,p,1}, b_{l,s,p,2}, \cdots, b_{l,s,p,K}\right]^T$, $p \in \{1, 2, \cdots, P\}$, K is the length of source information in a package, and N is the length of the corresponding encoded codeword. In the modulator, the encoded data stream $\mathbf{c}_{l,s}$ is modulated with constellation rotation. The output of the modulator is denoted by sequence $\mathbf{x}_{l,s} = \left[\mathbf{x}^T{}_{l,s,1}, \mathbf{x}^T{}_{l,s,2}, \ldots, \mathbf{x}^T{}_{l,s,P}\right]^T$, where $\mathbf{x}_{l,s,p} = \left[x_{l,s,p,1}, x_{l,s,p,2}, \cdots, x_{l,s,p,N}\right]^T$. Then each package of $\mathbf{x}_{l,s}$ is replicated M times and permuted with different interleavers, which produces the signal $\tilde{\mathbf{x}}_{l,s}$ composed of $\left\{\tilde{\mathbf{x}}^1_{l,s,1}, \cdots, \tilde{\mathbf{x}}^M_{l,s,1}, \cdots, \tilde{\mathbf{x}}^1_{l,s,P}, \cdots, \tilde{\mathbf{x}}^M_{l,s,P}\right\}$. The signal $\tilde{\mathbf{x}}_{l,s}$ is superimposed on other data streams to generate the signal $\mathbf{s}$ during the spatial coupling. We define the system described above as a (L, S, P, M)-multiuser spatial coupling structure.

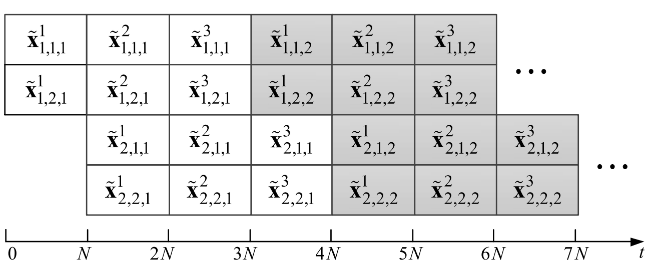

Fig. 2. Coupling of modulated data streams with time offset N in a $(2, 2, P, 3)$-multiuser spatial coupling structure.

$$\mathbf{H} = \begin{bmatrix}
\boldsymbol{\pi}^1_{1,1,1} & \cdots & \boldsymbol{\pi}^M_{1,1,1} & \cdots\cdots & \boldsymbol{\pi}^1_{1,1,P} & \cdots & \boldsymbol{\pi}^M_{1,1,P} & & & & & \\
\boldsymbol{\pi}^1_{1,2,1} & \cdots & \boldsymbol{\pi}^M_{1,2,1} & \cdots\cdots & \boldsymbol{\pi}^1_{1,2,P} & \cdots & \boldsymbol{\pi}^M_{1,2,P} & & & & & \\
\vdots & \cdots & \vdots & \cdots\cdots & \vdots & \cdots & \vdots & & & & & \\
\boldsymbol{\pi}^1_{1,S,1} & \cdots & \boldsymbol{\pi}^M_{1,S,1} & \cdots\cdots & \boldsymbol{\pi}^1_{1,S,P} & \cdots & \boldsymbol{\pi}^M_{1,S,P} & & & & & \\
& \boldsymbol{\pi}^1_{2,1,1} & \cdots & \boldsymbol{\pi}^M_{2,1,1} & \cdots\cdots & \boldsymbol{\pi}^1_{2,1,P} & \cdots & \boldsymbol{\pi}^M_{2,1,P} & & & & \\
& \boldsymbol{\pi}^1_{2,2,1} & \cdots & \boldsymbol{\pi}^M_{2,2,1} & \cdots\cdots & \boldsymbol{\pi}^1_{2,2,P} & \cdots & \boldsymbol{\pi}^M_{2,2,P} & & & & \\
& \vdots & \cdots & \vdots & \cdots\cdots & \vdots & \cdots & \vdots & & & & \\
& \boldsymbol{\pi}^1_{2,S,1} & \cdots & \boldsymbol{\pi}^M_{2,S,1} & \cdots\cdots & \boldsymbol{\pi}^1_{2,S,P} & \cdots & \boldsymbol{\pi}^M_{2,S,P} & & & & \\
& & \ddots & & \vdots & \cdots & \vdots & \cdots & \vdots & & & \\
& & & \boldsymbol{\pi}^1_{L,1,1} & \cdots & \boldsymbol{\pi}^M_{L,1,1} & \cdots\cdots & \boldsymbol{\pi}^1_{L,1,P} & \cdots & \boldsymbol{\pi}^M_{L,1,P} \\
& & & \boldsymbol{\pi}^1_{L,2,1} & \cdots & \boldsymbol{\pi}^M_{L,2,1} & \cdots\cdots & \boldsymbol{\pi}^1_{L,2,P} & \cdots & \boldsymbol{\pi}^M_{L,2,P} \\
& & & \vdots & \cdots & \vdots & \cdots\cdots & \vdots & \cdots & \vdots \\
& & & \boldsymbol{\pi}^1_{L,S,1} & \cdots & \boldsymbol{\pi}^M_{L,S,1} & \cdots\cdots & \boldsymbol{\pi}^1_{L,S,P} & \cdots & \boldsymbol{\pi}^M_{L,S,P}
\end{bmatrix} \tag{1}$$

Without loss of generality, we consider the $(2, 2, P, 3)$-multiuser spatial coupling structure. The spatial coupling procedure is represented in Fig. 2, where each row is a data stream of a user, and the packages are transmitted one after another. The block $\tilde{\mathbf{x}}^m_{l,s,p}$ can be denoted as $\tilde{\mathbf{x}}^m_{l,s,p} = \boldsymbol{\pi}^m_{l,s,p}\mathbf{x}_{l,s,p}$, where $\boldsymbol{\pi}^m_{l,s,p}$ is the corresponding interleaver. At time $t = 0$, two data streams of the first user start to transmit. The signal transmitted adds two data streams of the other user after N bit intervals in order.

We can also use spatial coupling matrix $\mathbf{H}$ to describe the above procedure. The construction of $\mathbf{H}$ is shown in (1), where $\boldsymbol{\pi}^m_{l,s,p}$ is the permutation of an $N \times N$ unit matrix. Therefore, the signal $\mathbf{s}$ can be described as $\mathbf{s} = \mathbf{H}^T\mathbf{x}$, where $\mathbf{x} = \left[\mathbf{x}^T{}_{1,1,1}, \cdots, \mathbf{x}^T{}_{1,1,P}, \cdots, \mathbf{x}^T{}_{L,S,1}, \cdots, \mathbf{x}^T{}_{L,S,P}\right]^T$. The load of the system we study is given in (2), which is actually the ratio of the numbers of rows and columns of $\mathbf{H}$.

$$Load = \frac{LSPN}{(PM + L - 1)N} = \frac{LSP}{PM + L - 1}. \tag{2}$$

Considering that the signal $\mathbf{s}$ is transmitted through the AWGN channel, the received signal $\mathbf{y}$ can be represented as

$$\mathbf{y} = \lambda\mathbf{s} + \mathbf{n}, \tag{3}$$

where λ is the power normalization coefficient, $\mathbf{n}$ is the complex Gaussian with zero mean and variance $\sigma^2/2$ for each dimension.

At the receiver, iterative detection and decoding based on message passing algorithm (MPA) is performed. Inner the spatial coupling structure, the extrinsic messages are iteratively exchanged along the edges between the channel nodes and the variable nodes. For the iteration between the detector and decoders, which is called outer iteration, and the output of the detector is transmitted to the decoders, the outputs of the decoders is used as the input of the detector for the next iteration. Note that each package of a data stream is encoded and decoded individually, and the maximum number of the outer iteration is defined as $I_{\max}$.

III. CONSTELLATION ROTATION IN SPATIAL COUPLING

A. Constellation rotation

For each data stream, the principle of constellation rotation is illustrated in Fig. 3, where the modulated signal is constructed by anticlockwise rotating the standard modulation with a certain angle θ, $\theta \in [0, 180)$.

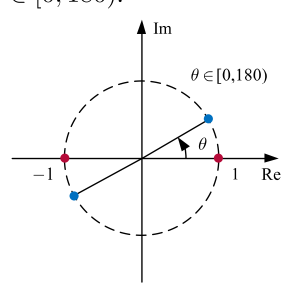

Fig. 3. The constellation rotation in the modulation.

Assuming that $\mathbf{x}'_{l,s}$ denotes the standard BPSK modulated symbol of $\mathbf{c}_{l,s}$, $\mathbf{x}'_{l,s} = \left[\mathbf{x}'^{T}{}_{l,s,1}, \mathbf{x}'^{T}{}_{l,s,2}, \cdots, \mathbf{x}'^{T}{}_{l,s,P}\right]^{T}$. Then the rotated symbol $\mathbf{x}_{l,s}$ with angle $\theta_{l,s}$ can be described as

$$\mathbf{x}_{l,s} = e^{i\theta_{l,s}} \mathbf{x}'_{l,s}. \tag{4}$$

B. Spatial coupling with constellation rotation

There exists inevitable interference when different signals are superimposed in the spatially-coupled multiuser transmission. Therefore, in this paper we introduce the constellation rotation to make a further distinction between the superimposed signals. It diversifies the constellation of the coupled signal $\mathbf{s}$ and contributes to the performance improvement of the system. The constellation rotation can be carried out in the following two manners.

(I) We only deal with the interferences between the data streams of the same user by rotating them with different angles. The same rotating rule is applied on all the users.

(II) To further distinguish the interferences between different users, we can use different angles to modulate all different data streams. This expands the diversity of the constellation at the cost of increasing the implementation complexity.

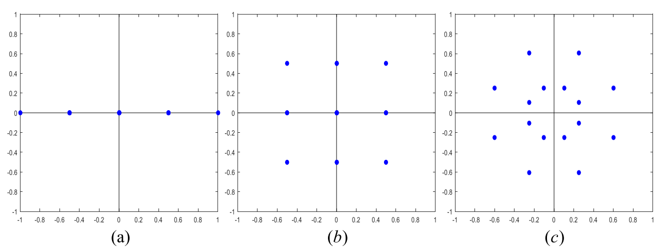

Fig. 4. The constellations of coupled signal $\mathbf{s}$ in the $(2, 2, P, S)$-multiuser spatial coupling system. Rotation angle sets from left to right are $(0, 0, 0, 0)$, $(0, 90, 0, 90)$ and $(0, 90, 45, 135)$, respectively. $(0, 90, 45, 135)$ is the optimal angle set.

We take the $(2, 2, P, S)$-multiuser spatial coupling system as observation, and the constellations of $\mathbf{s}$ with different rotation angle sets are shown in Fig. 4. As can be seen from the figure, the constellation of $\mathbf{s}$ may contain 16 points when all data streams are modulated with different angles. There may exist constellation overlapping when different users employ the same rotation rule. We call this phenomenon constellation aliasing. Nonetheless, both of them obtain higher diversity in constellation compared with the constellation without any rotation.

When considering constellation, we naturally come up with the minimum Euclidean distance which reflects the distinction between constellation points. The minimum Euclidean distance decreases when the diversity of the constellation increases. Therefore, it is necessary to make a trade-off between the diversity and the distinction and search for the optimal rotation angles.

C. Rotation angle optimization

The optimization of rotation angles can be carried out by maximizing the average mutual information between the input $\mathbf{S}$ and the output $\mathbf{Y}$. The maximum AMI represents the maximum amount of information about $\mathbf{S}$ that can be conveyed through the channel. We denote the constellation point set of $\mathbf{S}$ by $\{\hat{s}_t\}, t \in \{1, 2, \cdots, T = 2^{LS}\}$, $\hat{s}_t = a_t + ib_t$, and y represents the element in $\mathbf{Y}$, $y = u + iv$. Then the channel transition probability density is given as

$$p(y|\hat{s}_t) = \frac{1}{\pi N_0} e^{-\frac{(u-a_t)^2}{N_0} - \frac{(v-b_t)^2}{N_0}} = \frac{1}{\pi N_0} e^{-\frac{|y-\hat{s}_t|^2}{N_0}}, \tag{5}$$

where N_0 is the noise power spectral density. The formula of the AMI is given as

$$I(\mathbf{S}; \mathbf{Y}) = \sum_{t=1}^{T} p(\hat{s}_t) \int p(y|\hat{s}_t) \log \frac{p(y|\hat{s}_t)}{\sum_{t'=1}^{T} p(\hat{s}_{t'}) p(y|\hat{s}_{t'})} dy, \tag{6}$$

As $\hat{s}_t$ occurs with equal probability, we combine (5) and (6) and get

$$I(\mathbf{S}; \mathbf{Y}) = \log T - \frac{1}{T} \sum_{t=1}^{T} \int \frac{1}{\pi N_0} e^{-\frac{|y-\hat{s}_t|^2}{N_0}} \log \sum_{t'=1}^{T} e^{-\frac{|y-\hat{s}_{t'}|^2 - |y-\hat{s}_t|^2}{N_0}} dy. \tag{7}$$

The maximization of the AMI can be done through traversing all sets of rotation angles when the total number of data streams LS is determined. The symmetry of the constellation can be employed to reduce the searching complexity.

D. Iterative detection and decoding

In this section, we describe the process of iterative detecting and decoding in detail. During the detection, the log-likelihood ratios (LLRs) are used as the extrinsic information and passed between nodes given in Fig. 5. The received message of one node along one edge is not allowed to update the message sent from the same edge.

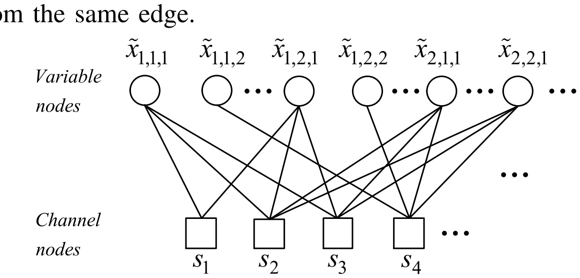

Fig. 5. Factor graph representation of spatial coupling multiple access system, where circles represent variable nodes corresponding to the data blocks in Fig. 2, while channel nodes are coupled data and denoted by squares.

Take the edge between variable node $\tilde{x}_{l,s,p}$ and channel node s_t as observation. Set $\xi(l, s, p)\backslash t$ as the index collection of channel nodes connected with variable node $\tilde{x}_{l,s,p}$ and set $\zeta t\backslash(l, s, p)$ as the index collection of variable nodes connected with channel nodes s_t. Symbols $l_{\tilde{x}_{l,s,p}\to s_t}$ and $l_{s_t\to\tilde{x}_{l,s,p}}$ represent the messages sent from $\tilde{x}_{l,s,p}$ and s_t, respectively. We initialize $l_{\tilde{x}_{l,s,p}\to s_t}$ as

$$l_{\tilde{x}_{l,s,p}\to s_t} = \log \frac{p(\tilde{x}_{l,s,p} = +e^{i\theta_{l,s}})}{p(\tilde{x}_{l,s,p} = -e^{i\theta_{l,s}})}. \tag{8}$$

The message updated during the iteration can be written as

$$l_{\tilde{x}_{l,s,p}\to s_t} = \sum_{t' \in \xi(l,s,p)\backslash t} l_{s_{t'}\to\tilde{x}_{l,s,p}}, \tag{9}$$

$$l_{s_t \to \tilde{x}_{l,s,p}} = \log \frac{p(\tilde{x}_{l,s,p} = +e^{i\theta_{l,s}} | s_t, \tilde{\mathbf{x}}^{[t]} \backslash \tilde{x}_{l,s,p})}{p(\tilde{x}_{l,s,p} = -e^{i\theta_{l,s}} | s_t, \tilde{\mathbf{x}}^{[t]} \backslash \tilde{x}_{l,s,p})}$$
$$= \log \frac{p(s_t | \tilde{\mathbf{x}}^{[t]}, \tilde{x}_{l,s,p} = +e^{i\theta_{l,s}}) p(\tilde{\mathbf{x}}^{[t]} | \tilde{x}_{l,s,p} = +e^{i\theta_{l,s}})}{p(s_t | \tilde{\mathbf{x}}^{[t]}, \tilde{x}_{l,s,p} = -e^{i\theta_{l,s}}) p(\tilde{\mathbf{x}}^{[t]} | \tilde{x}_{l,s,p} = -e^{i\theta_{l,s}})}, \tag{10}$$

where $\tilde{\mathbf{x}}^{[t]}$ denotes the set containing all signals superimposed on the coupled signal s_t. Equation (10) is derived by using Bayes' rule listed below

$$p(x|y) = \frac{p(y|x)p(x)}{p(y)} \propto p(y|x)p(x). \tag{11}$$

The conditional probability density function (pdf) of the coupled signal s_t and the set $\tilde{\mathbf{x}}^{[t]}$ are given separately as

$$p\left(s_t | \tilde{\mathbf{x}}^{[t]}\right) = \frac{1}{\sqrt{2\pi}\sigma} \exp\left(-\frac{1}{2\sigma^2} \left\| s_t - \mathbf{h}^{[t]T} \tilde{\mathbf{x}}^{[t]} \right\|^2\right), \tag{12}$$

and

$$p\left(\tilde{\mathbf{x}}^{[t]} | \tilde{x}_{l,s,p}\right) = \prod_{(l',s',p') \in \zeta t \backslash (l,s,p)} p(\tilde{x}_{l',s',p'}), \tag{13}$$

where $\mathbf{h}^{[t]}$ is the normalized coefficient vector of $\tilde{\mathbf{x}}^{[t]}$. The symbol $\|\|$ denotes modulus operation and the *a priori* probability of $\tilde{x}_{l',s',p'}$ is written as

$$p(\tilde{x}_{l',s',p'}) = \exp\left(\frac{\tilde{x}_{l',s',p'}}{2} l_{\tilde{x}_{l',s',p'} \to s_t}\right). \tag{14}$$

Substituting (12), (13) and (14) into (10), we get (15) shown on the top of next page, where $\max^*$ operation [11] is defined as

$$\begin{aligned} \max{}^*(a,b) &= \log(\exp(a) + \exp(b)) \\ &= \max(a,b) + \log(1 + \exp(-|a-b|)). \end{aligned} \tag{16}$$

We define the iterative process from the detector to the decoders as a complete iteration. The message exchanged between the detector and the decoders can be described as

$$l_{out,\tilde{x}_{l,s,p}}^{DEC[i]} = l_{\tilde{x}_{l,s,p}}^{I_{DEC}} - l_{out,\tilde{x}_{l,s,p}}^{DET[i]}, \tag{17}$$

where the symbol on the left side of the equation represents the output of the decoder in the i-th iteration, $i \in \{1, \cdots I_{\max}\}$. On the right side, the minuend is the LLR of the decoder after I_{DEC} inner iterations and is used for soft decision. The subtrahend denotes the output of the detector in i-th iteration, initialized as 0 when $i = 1$ and is updated as

$$l_{out,\tilde{x}_{l,s,p}}^{DET[i]} = l_{\tilde{x}_{l,s,p}}^{I_{DET}} - l_{out,\tilde{x}_{l,s,p}}^{DEC[i-1]}, \tag{18}$$

where $l_{\tilde{x}_{l,s,p}}^{I_{DET}}$ is the total LLR received from neighbors of $\tilde{x}_{l,s,p}$ after I_{DET} inner iterations. The symbol $l_{out,\tilde{x}_{l,s,p}}^{DEC[i-1]}$ is the $(i-1)-$th iterative output of the detector.

IV. SIMULATION RESULTS AND DISCUSSIONS

In this section, we analyze the system performance using EXIT charts and BER curves. The system parameters are configured as follows. The encoding scheme considered in the paper is the $(3,6)$-regular LDPC code with length $N = 1800$ and rate $1/2$.

A. EXIT charts

The EXIT chart is a useful tool to track the mutual information at each iteration in a soft-in soft-out (SISO) system, and it provides an excellent prediction on the behavior of the detecting and/or the decoding. We use the EXIT chart to evaluate the performance of the detector (or decoders) by observing whether it is conductive to increase the output mutual information I_E when the input extrinsic information I_A is given.

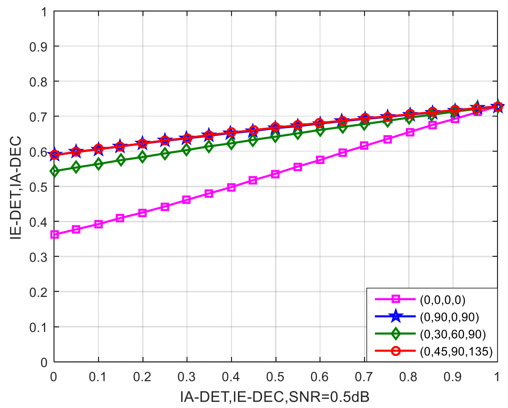

Fig. 6. The EXIT curve of the detector with different rotation angle set in the $(2,2,5,2)$-multiuser spatial coupling structure with SNR = 0.5dB.

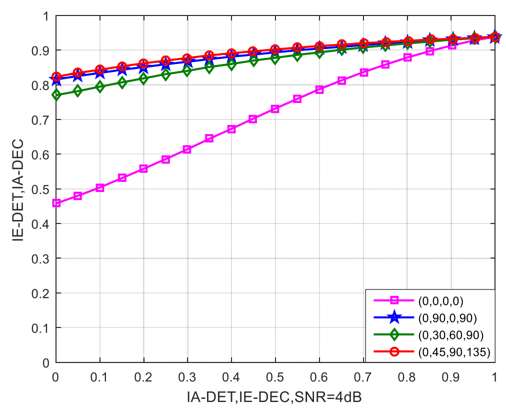

Fig. 7. The EXIT curves of the detector with different rotation angle sets in the $(2,2,5,2)$-multiuser spatial coupling structure with SNR = 4dB.

We take the $(2,2,5,2)$-multiuser spatial coupling structure as an instance. Two EXIT curves of detector with different rotation angle sets over AWGN channels are provided for SNR = 0.5dB in Fig. 6 and SNR = 4dB in Fig. 7. According to the figures, we reach a conclusion that the constellation rotation does contribute to increase the output mutual information of the detector. When we only consider the interferences between two data streams of the same user, the optimal rotation angle set is $(0,90,0,90)$, namely, two data streams of each user are orthogonal to each other. That means there exists no interference between certain user's different data streams. However, the interferences between the two users can not be eliminated and result in the constellation aliasing. When all data streams are taken into account, the diversity of constellation increases. In this case, the optimal rotation angle set we seek out is $(0,90,45,135)$. It can be seen that when the SNR is 0.5dB, the performance of the detector for $(0,90,45,135)$ is almost

$$
\begin{aligned}
l_{s_t \to \tilde{x}_{l,s,p}} = & \max_{\substack{\tilde{\mathbf{x}}^{[t]} \\ \tilde{x}_{l,s,p} = +e^{i\theta_{l,s}}}}^{\star} \left(\sum_{(l',s',p') \in \zeta t \setminus (l,s,p)} \frac{\tilde{x}_{l,s,p}}{2} l_{\tilde{x}_{l,s,p} \to s_t} - \frac{1}{2\sigma^2} \left\| s_t - \mathbf{h}^{[t]T} \tilde{\mathbf{x}}^{[t]} \right\|^2 \right) \\
- & \max_{\substack{\tilde{\mathbf{x}}^{[t]} \\ \tilde{x}_{l,s,p} = -e^{i\theta_{l,s}}}}^{\star} \left(\sum_{(l',s',p') \in \zeta t \setminus (l,s,p)} \frac{\tilde{x}_{l,s,p}}{2} l_{\tilde{x}_{l,s,p} \to s_t} - \frac{1}{2\sigma^2} \left\| s_t - \mathbf{h}^{[t]T} \tilde{\mathbf{x}}^{[t]} \right\|^2 \right).
\end{aligned}
\tag{15}
$$

the same as that for $(0, 90, 0, 90)$. That is to say that the interference plays a dominant role in the factors affecting the performance rather than diversity. On the contrary, when the SNR is 4dB, the performance of the detector is better for $(0, 90, 45, 135)$, which means the diversity is the main influencing factor. Anyway, both of them clearly outperform the systems with rotation angle sets randomly selected, such as $(0, 30, 60, 90)$.

B. BER curves

We have demonstrated that the constellation rotation is applicable to any spatial coupling multiuser transmission structure. In this subsection, we take the $(2, 2, 5, 2)$-multiuser spatial coupling structure and the $(3, 2, 6, 3)$-multiuser spatial coupling structure as examples. The optimal rotation angle sets we obtain are $(0, 90, 45, 135)$ and $(0, 90, 30, 120, 60, 150)$, respectively.

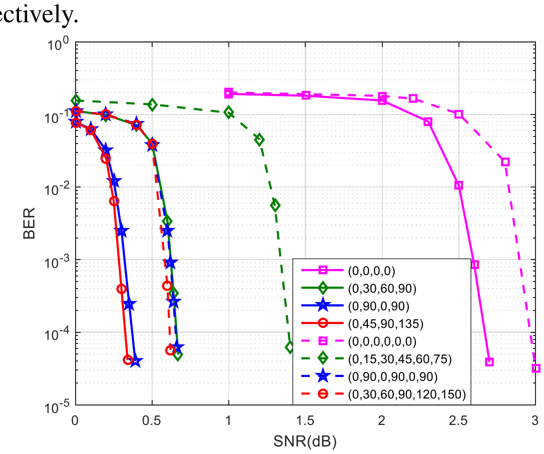

Fig. 8. The average BER curves of different spatially-coupled multiuser transmission systems with different rotation angle sets.

We illustrate the average BER curves of the system in Fig. 8, where solid and dotted curves represent the systems with the structure $(2, 2, 5, 2)$ and the structure $(3, 2, 6, 3)$, respectively. It can be observed that the system with constellation rotation achieves the better performance. Meanwhile, the optimal rotation angle sets we have found out outperform the others in terms of BER performance, which is consistent with the analysis of EXIT charts. In addition, the performance of the system with constellation rotation converges faster, which is beneficial to reduce the decoding complexity and latency of the system.

V. CONCLUSIONS

In this paper, we have introduced constellation rotation into spatially-coupled multiuser transmission to mitigate the interferences between data streams. We have also sought out the optimal rotation angle set by maximizing the average mutual information. The EXIT charts and BER simulation results verify that the constellation rotation generally improves the system performance and reduces the decoding complexity and latency. The system with the optimal rotation angle set performs better than the others.

ACKNOWLEDGEMENT

The work was supported in part by the National Natural Science Foundation of China (No.61401037), the Beijing Nova Program (No. Z171100001117049), and the Beijing Natural Science Foundation (No. 4162044).

REFERENCES

[1] L. Dai, B. Wang, Y. Yuan, S. Han, C. l. I and Z. Wang, “Non-orthogonal multiple access for 5G: solutions, challenges, opportunities, and future research trends,” in IEEE Communications Magazine, vol. 53, no. 9, pp. 74-81, September 2015.

[2] C. Yan, A. Harada, A. Benjebbour, Y. Lan, A. Li and H. Jiang, “Receiver Design for Downlink Non-Orthogonal Multiple Access (NOMA),” 2015 IEEE 81st Vehicular Technology Conference (VTC Spring), Glasgow, 2015, pp. 1-6.

[3] M. R. Hojeij, J. Farah, C. A. Nour and C. Douillard, “Resource Allocation in Downlink Non-Orthogonal Multiple Access (NOMA) for Future Radio Access,” 2015 IEEE 81st Vehicular Technology Conference (VTC Spring), Glasgow, 2015, pp. 1-6.

[4] D. Truhachev, M. Lentmaier and K. S. Zigangirov, “Mathematical analysis of iterative decoding of LDPC convolutional codes,” Proceedings. 2001 IEEE International Symposium on Information Theory (IEEE Cat. No.01CH37252), Washington, DC, 2001, pp. 191.

[5] M. Lentmaier, A. Sridharan, D. J. Costello and K. S. Zigangirov, “Iterative Decoding Threshold Analysis for LDPC Convolutional Codes,” in IEEE Transactions on Information Theory, vol. 56, no. 10, pp. 5274-5289, Oct. 2010.

[6] D. Truhachev, “Universal multiple access via spatially coupling data transmission,” 2013 IEEE International Symposium on Information Theory, Istanbul, 2013, pp. 1884-1888.

[7] K. Takeuchi, T. Tanaka and T. Kawabata, “Performance Improvement of Iterative Multiuser Detection for Large Sparsely Spread CDMA Systems by Spatial Coupling,” in IEEE Transactions on Information Theory, vol. 61, no. 4, pp. 1768-1794, April 2015.

[8] C. Schlegel and D. Truhachev, “Multiple Access Demodulation in the Lifted Signal Graph With Spatial Coupling,” in IEEE Transactions on Information Theory, vol. 59, no. 4, pp. 2459-2470, April 2013.

[9] R. Zhang and L. Hanzo, “A Unified Treatment of Superposition Coding Aided Communications: Theory and Practice,” in IEEE Communications Surveys & Tutorials, vol. 13, no. 3, pp. 503-520, Third Quarter 2011.

[10] D. Cai, P. Fan, X. Lei, Y. Liu and D. Chen, “Multi-Dimensional SCMA Codebook Design Based on Constellation Rotation and Interleaving,” 2016 IEEE 83rd Vehicular Technology Conference (VTC Spring), Nanjing, 2016, pp. 1-5.

[11] R. Hoshyar, F. P. Wathan and R. Tafazolli, “Novel Low-Density Signature for Synchronous CDMA Systems Over AWGN Channel,” in IEEE Transactions on Signal Processing, vol. 56, no. 4, pp. 1616-1626, April 2008.